NASA TECHNICAL MEMORANDUM

NASA TM X-1964

NASA TM X-1964

COMPUTER STUDY OF A DEAD-BAND CONDENSING-PRESSURE CONTROL FOR SNAP-8 STARTUP

by Roy C. Tew and James D. Gallagher

Lewis Research Center
Cleveland, Ohio

NATIONAL AERONAUTICS AND SPACE ADMINISTRATION • WASHINGTON, D. C. • FEBRUARY 1970

1. Report No. NASA TM X-1964	2. Government Accession No.	3. Recipient's Catalog No.
4. Title and Subtitle COMPUTER STUDY OF A DEAD-BAND CONDENSING-PRESSURE CONTROL FOR SNAP-8 STARTUP		5. Report Date February 1970
		6. Performing Organization Code
7. Author(s) Roy C. Tew and James D. Gallagher		8. Performing Organization Report No. E-5384
9. Performing Organization Name and Address Lewis Research Center National Aeronautics and Space Administration Cleveland, Ohio 44135		10. Work Unit No. 120-27
		11. Contract or Grant No.
12. Sponsoring Agency Name and Address National Aeronautics and Space Administration Washington, D.C. 20546		13. Type of Report and Period Covered Technical Memorandum
		14. Sponsoring Agency Code

15. Supplementary Notes

16. Abstract

A digital-computer simulation of the SNAP-8 space power system was used to evaluate a method for condensing-pressure control during system startup. Mercury-condensing pressure is controlled by varying the condenser-coolant (NaK) flow rate whenever the pressure goes outside a dead-band. Control parameters studied were (1) pressure dead-band width, (2) valve gain defined as rate of change of flow over flow, and (3) initial coolant flow through the condenser. System characteristics studied were (1) the amount of mercury that accumulates in the condenser and (2) the mercury-flow ramp rate.

17. Key Words (Suggested by Author(s))	18. Distribution Statement
Condensing pressure control Rankine cycle power system Digital computer simulation	Unclassified - unlimited

19. Security Classif. (of this report)	20. Security Classif. (of this page)	21. No. of Pages	22. Price*
Unclassified	Unclassified	28	$3.00

*For sale by the Clearinghouse for Federal Scientific and Technical Information
Springfield, Virginia 22151

COMPUTER STUDY OF A DEAD-BAND CONDENSING-PRESSURE CONTROL FOR SNAP-8 STARTUP

by Roy C. Tew and James D. Gallagher

Lewis Research Center

SUMMARY

A digital-computer simulation of the SNAP-8 space power system was used to evaluate a dead-band method of controlling condensing pressure during the startup transients. With this control method, the mercury-condensing pressure is controlled by varying the condenser-coolant flow rate whenever pressure goes outside some predetermined dead-band. Increasing the coolant flow, for example, tends to increase the rate of heat extraction from the condenser and therefore to decrease the condensing pressure. Since the condensing pressure is also the turbine back-pressure, high pressures must be prevented so as not to excessively lower turbine output power. And, since the mercury pump net positive suction head (NPSH) is maintained by the condensing pressure and the amount of subcooling, it is equally important to avoid excessively low pressure throughout startup in order to prevent the pump from cavitating.

The study covered a range of values for each of the following control parameters: (1) pressure dead-band width, (2) rate of change of coolant flow, and (3) initial coolant flow through the condenser. The study also covered a range of values for each of the following system characteristics: (1) the amount of mercury that accumulates in the condenser (condenser inventory); and (2) the mercury-flow ramp rate, which determines the rate of buildup of the mercury liquid-vapor interface in the condenser.

In addition to detailed information on the control characteristics, the study produced the following results concerning the sensitivity of control performance to system characteristics:

(1) There is a limited range of inventories for which control performance is satisfactory.

(2) Mercury-flow ramps to the system self-sustaining level from 40 to 100 seconds in duration should allow satisfactory control performance (provided condenser inventory is within the correct range).

INTRODUCTION

SNAP-8 is a 35-kilowatt electric nuclear Rankine-cycle space power system currently under development. It has three liquid-metal heat-transfer loops and a lubricant-coolant loop. (A schematic diagram showing the three liquid metal heat transfer loops is shown in fig. 1.) In the first loop NaK, the eutectic mixture of sodium and potassium, is circulated to transfer heat from the nuclear reactor to the mercury boiler. The second loop is the mercury Rankine loop. In this loop, liquid mercury is heated, evaporated, and superheated in a counterflow multitube boiler. After passing through the turboalternator, the mercury is condensed and subcooled in a counterflow multitube condenser. The third loop, the heat-rejection loop, circulates NaK to transfer heat from the condenser to the radiator, where it is dissipated to space. The fourth loop circulates oil in order to cool and lubricate the turboalternator and the motor-driven mercury pump. This electric generating system is being developed to operate unattended for at least 10 000 hours in space after automatic startup. It will also have shutdown and restart capabilities.

The startup of SNAP-8 has two phases: (1) reactor startup during which the primary loop is brought to design temperature; and (2) power-conversion system startup during which self-sustaining operation and, subsequently, full-power operation is attained. At the beginning of the second phase, the mercury inventory is injected into the evacuated second loop in accordance with a programmed ramp of flow rate as a function of time so that the turboalternator is brought to rated speed. When the injection process is complete, the mercury pump recirculates the liquid mercury from the condenser back to the boiler. When the system reaches the self-sustaining power level, the mercury flow rate is held constant until transients have settled out; it is then increased in a gradual manner to the full-power value.

During power conversion system startup, the condensing pressure should vary smoothly from essentially zero to the design value. There may be transient conditions, however, which will tend to cause the pressure to rise much higher than the design value (14.0 psi, 9.66 N/cm^2). These high pressures will occur if the NaK flowing through the condenser is too low relative to the heat input from the mercury loop. And, since the condensing pressure is also the turbine backpressure, pressures much higher than 15.0 or 16.0 psi (10.3 or 11.0 N/cm^2) should be avoided so as not to lower the turbine output power, especially when the turbine is accelerating. A very high condensing pressure could also exceed the condenser structural design limit (60.0 psi, 41.4 N/cm^2). It is also important to have sufficient condensing pressure throughout startup to prevent the mercury pump from cavitating. This is especially important under zero-gravity conditions, for which the pump net positive suction head (NPSH) is maintained by a combination of condensing pressure and subcooling. Too low a pressure will reduce the pump suction head below the level required to prevent cavitation. Therefore, some form

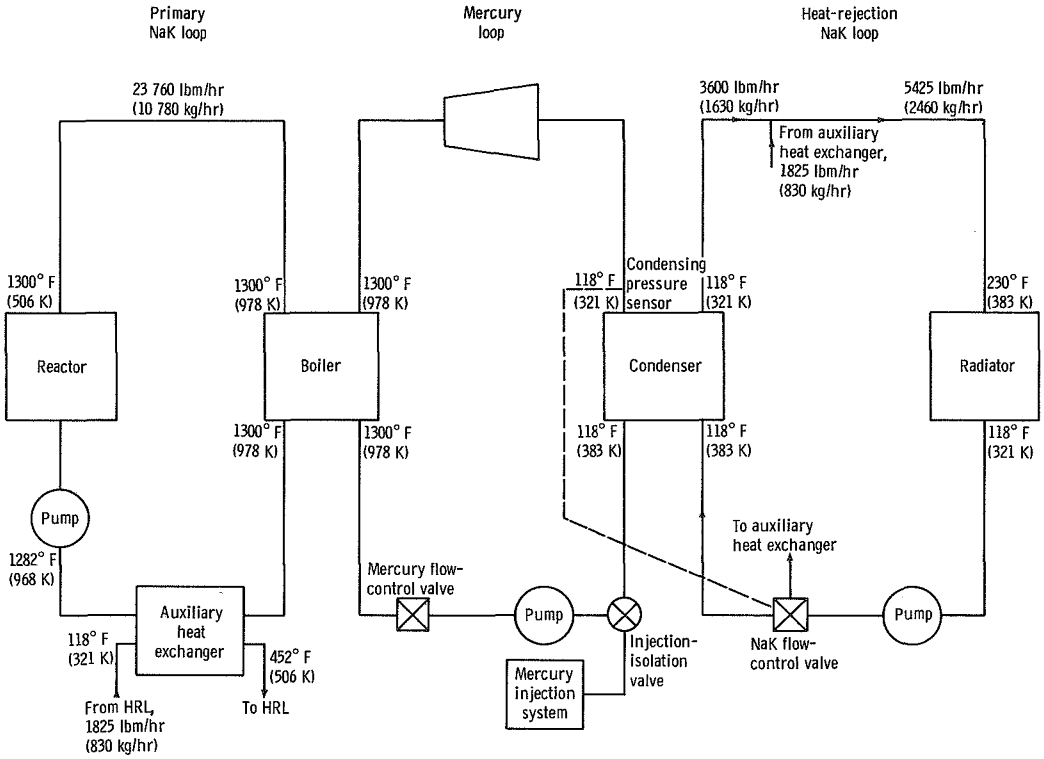

(a) Initial conditions for mercury loop startup.

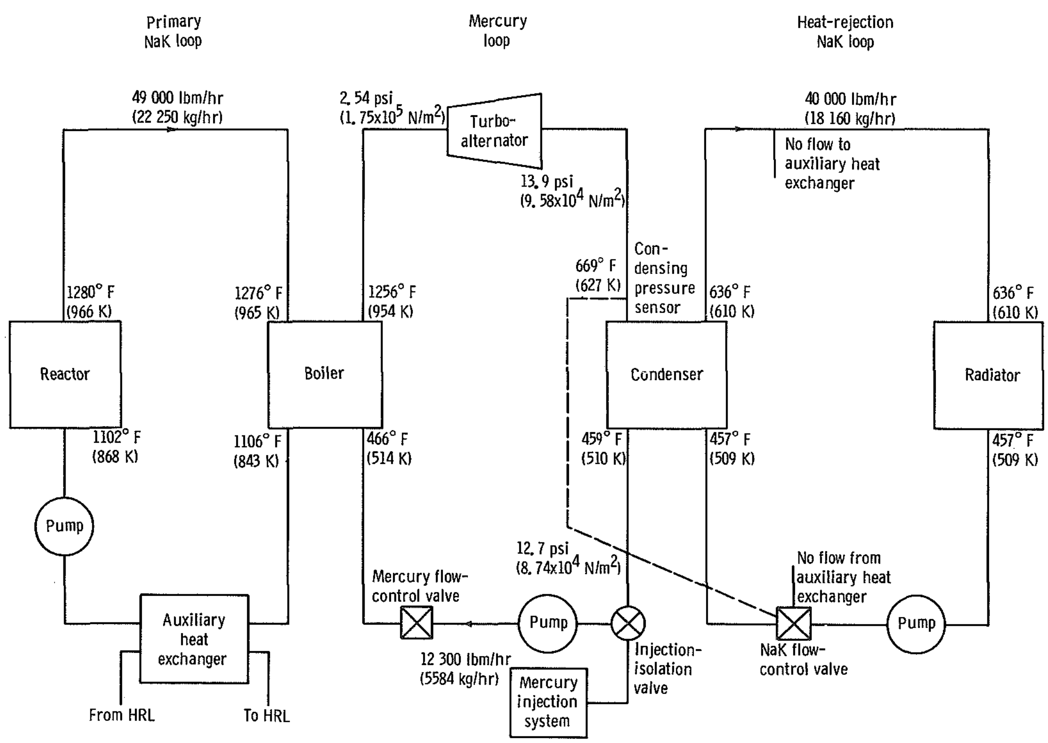

(b) Conditions at design operating point.

Figure 1. - System conditions.

of pressure control is required to avoid the operating problems associated with these two extremes of condenser pressure.

This study is an evaluation of a dead-band method of controlling the mercury-condensing pressure during startup. With this method, the condensing pressure is controlled by varying the NaK coolant flow rate through the condenser whenever the condensing pressure goes outside some predetermined dead-band. If, for example, the condensing pressure exceeds the upper dead-band limit, the coolant flow increases. The increased coolant flow increases the rate of heat extraction from the condenser and tends to reduce the condensing pressure. The coolant flow continues to increase until the pressure drops below the upper dead-band limit.

In reference 1, condensing-pressure control for long-term operation of the SNAP-8 system was studied. This study indicated that variations of condensing pressure around the design operating point could be expected, and methods of controlling these variations were investigated. One of the methods investigated was a dead-band control, and the results indicated that this method of control could be used successfully. These studies, however, were made only for pressure variations around the design operating point. The analysis herein treats the more critical variations occurring during the startup transient.

The study was made by using a digital-computer simulation of the SNAP-8 system; it covered a range of values for each of the following control parameters: (1) pressure dead-band width, (2) a valve gain defined as rate of change of flow over flow, and (3) initial coolant flow through the condenser. Since the inventory in the condenser strongly affects the condensing pressure, runs were made for a range of condenser inventories (i.e., by varying the amount of mercury injected into the system). The effect of mercury flow rate schedule was investigated by using two different mercury ramps to the self-sustaining level.

DESCRIPTION OF DIGITAL COMPUTER SIMULATION

The following major components of the SNAP-8 system were included in the digital computer dynamic simulation: boiler, turbine, alternator (and the associated electrical components), condenser, radiator, auxiliary start heat exchanger, heat-rejection loop, auxiliary start loop, flow-control valve, and all the pipe lines between these components. A reactor simulation was not used; therefore, the temperature of the NaK coming into the boiler was assumed to stay at the design value for all startup runs evaluated. (Expected variations in boiler inlet temperature during startup should not significantly affect condenser input variables.)

Condenser Simulation

In the SNAP-8 condenser, the mercury flows axially in 73 inner tubes, while the NaK flows through the shell counterflow to the mercury. The tubes are tapered to maintain vapor velocity which provides a continual movement of condensate to the liquid-vapor interface in zero-gravity operation. A detailed description of this condenser and its steady-state performance is given in reference 2. Since the results used in this study depend heavily upon the condenser simulation, this simulation is described in detail in appendix A.

Description of Control Logic

Prior to mercury injection there is an initial NaK flow rate through the condenser, and the flow through the auxiliary start loop is at a value necessary to remove heat from the first loop for reactor startup. The auxiliary start loop includes the NaK flow path from the flow control valve to the auxiliary heat exchanger and back to the heat rejection loop (see fig. 1). During the preinjection period NaK flows are maintained by running the pumps on a battery-powered inverter at half design speed. The pumps are brought to design speed by switching them from the inverter to the alternator when the turbine speed passes through its half design speed level; thus, the pumps are said to be bootstrapped to their design level. In the simulation, the primary loop, heat-rejection loop (HRL), and auxiliary start loop (ASL) flows are bootstrapped at a rate proportional to the turbine speed from the time the turbine passes through its half design speed level. Therefore, the initial NaK flow at design pump speed is two times the initial NaK flow before bootstrapping. The flows are then kept at these levels during mercury injection until the condensing pressure exceeds some predetermined upper limit (the upper dead-band limit). At this time, both HRL and ASL flows are varied simultaneously in a manner such that the percentage change in flows with respect to time is constant. The flow through the condenser is increased as the ASL flow is decreased until either the condensing pressure drops below the upper dead-band limit or the design flow rate is reached. The flows do not change when the condensing pressure is within the dead-band. However, if the pressure goes below some predetermined lower limit (the lower dead-band limit), the flow through the condenser is decreased and the ASL flow is increased until either the pressure goes back above the lower dead-band limit or the condenser flow reaches the initial value for design pump speed. Therefore, this initial value of condenser flow is also the minimum flow; it is determined by the setting of the flow-control valve prior to mercury injection. (The flow returned to the initial (minimum) value for only one of the runs discussed.)

The simulated flow-control valve produces the same rate of change of flow over flow regardless of the flow rate; that is, the ratio $(1/w) \times (dw/dt)$ is constant, but the differential dw/dt (rate of change of flow rate) increases as the flow increases. The total heat-rejection-loop flow is the sum of the condenser coolant flow and the ASL flow. The rate of change of flow over flow for the condenser coolant flow and for the ASL flow are equal in magnitude but opposite in sign. The magnitude of this flow parameter can be considered the flow-control-valve gain; it will be referred to as such from now on.

The value of the condensing pressure is obtained from the condenser simulation and is used together with a first-order lag (with a time constant of 0.1 sec, which was included to simulate pressure sensor dynamics).

Procedures for Making Startup Runs

The initial conditions for all three loops, prior to mercury loop startup, are shown in the schematic diagram in figure 1(a) for condenser NaK flow equal to 9 percent of the design flow. For the case shown, the initial condenser flow (and the minimum flow) after bootstrapping of the pumps to design speed would be 18 percent of the design flow. In the first loop the NaK flow rate is at 50 percent of design value, the boiler is at a uniform temperature of 1300° F, and the auxiliary-start heat exchanger is extracting heat from the primary NaK loop. In the third loop the temperatures are determined by the NaK flow rate, the heat coming from the auxiliary start loop, and the radiator characteristics. The flow through the condenser keeps it at a uniform temperature equal to the radiator exit temperature. System conditions at the design operating point are shown in figure 1(b). For one group of startup runs, the mercury flow rate schedule (as seen at the boiler inlet) was as follows: (1) a ramp from zero to 53.5 percent of design flow rate in 100 seconds; (2) remained at 53.5 percent of design flow. This flow rate schedule is shown in figure 2(a), and it will be referred to as the slow injection schedule or the slow ramp rate from now on. It should be pointed out that 53.5 percent of design flow rate is the minimum value needed for self-sustaining operation of the system; that is, operation with enough turboalternator electrical power to run the pumps and control components. For other startup runs the mercury was ramped from zero to 53.5 percent of design flow rate in 40 seconds, and then remained at 53.5 percent until the end of the run. This injection schedule will be referred to as the fast injection schedule or the fast ramp rate from now on (fig. 2(b) solid curve). The dashed curve in figure 2(b) indicates the form (but not necessarily the correct time intervals) that the complete mercury flow schedule is expected to have during startup of the SNAP-8 system. The slow ramp from 53.5 percent of design flow to design flow was not covered in the computer study. The slow transients resulting from this ramp were not expected to present a problem for the control and would, if studied, require a relatively large amount of computer time.

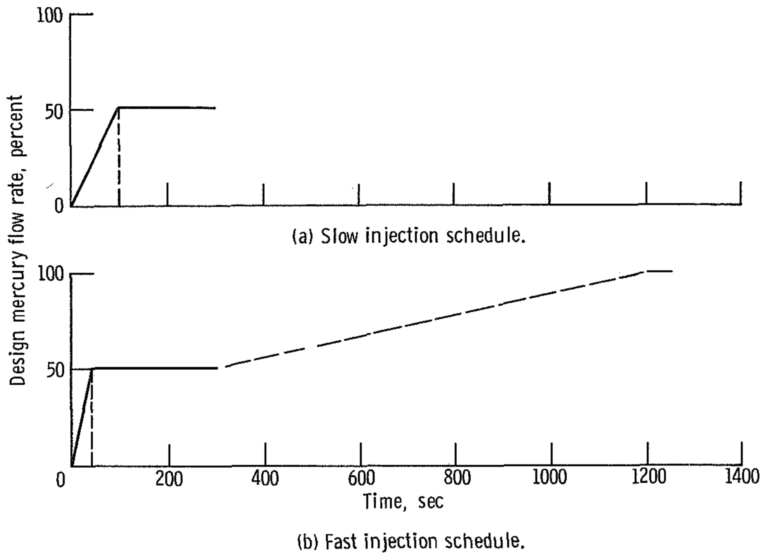

Figure 2. - Mercury injection schedules for startup.

For a given mercury flow rate schedule, the injection process continued until the mercury injected was sufficient to give the desired condenser inventory. At the same time that the injection process was stopped, the isolation valve (fig. 1) was opened to allow mercury to flow from the condenser to the mercury pump. The mercury injection-isolation valve was located at the exit to the condenser. The line between this valve and the pump, the pump, and the line between the pump and the flow-control valve (which was located at the boiler inlet) were assumed to have been prefilled.

RESULTS AND DISCUSSION

Effect of Pressure Dead-Band Width and Valve Gain

Pressure dead-band width and valve gain are considered together because both variables significantly affect the stability of the control. It is desirable to have the smallest dead-band and the highest gain consistent with stable operation of the control. Decreasing the dead-band width increases confidence that the condensing pressure is within an acceptable range (within the limits of stable operation). However, decreasing the dead-band width also makes the response of condensing pressure more oscillatory. Increasing the valve gain makes the control respond faster (thus decreasing overshoot of the dead-band limits) but also makes condensing-pressure response more oscillatory. The runs discussed allow approximate determination of the smallest dead-band width and the highest valve gain consistent with stable operation of the control.

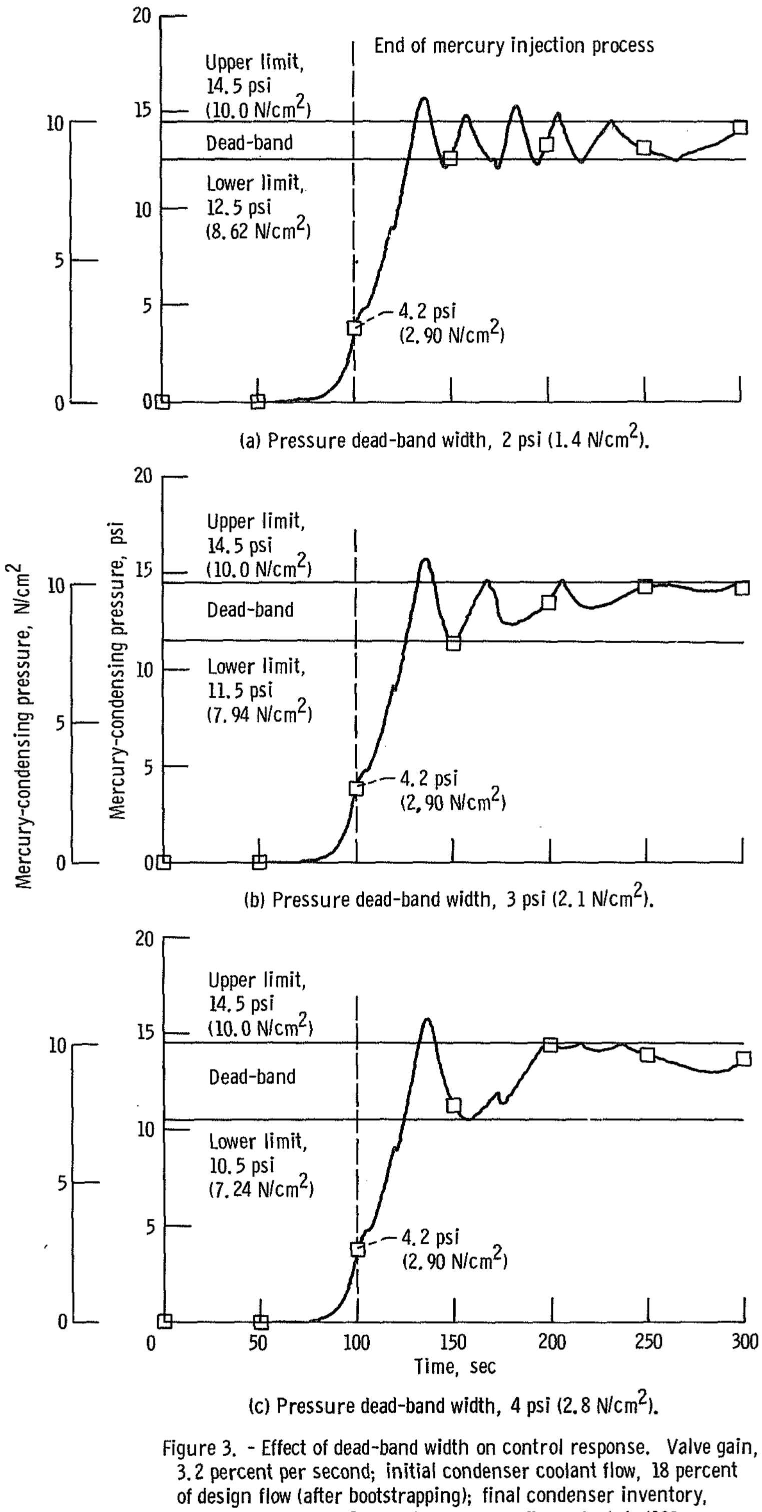

Figure 3. - Effect of dead-band width on control response. Valve gain, 3.2 percent per second; initial condenser coolant flow, 18 percent of design flow (after bootstrapping); final condenser inventory, 40 pounds mass (18.2 kg); slow mercury flow schedule (100-sec ramp).

For all startup runs discussed in this section, the slow mercury flow schedule (100-sec ramp) was used and the final condenser inventory was 40 pounds (18 kg).

In figure 3 mercury-condensing-pressure variations for startup runs with three different pressure dead-band widths are shown. For all three runs the valve gain was 3.2 percent change in flow per second and the NaK flow, immediately after bootstrapping, was 18 percent of the design flow. (The NaK flow was 9 percent of design flow before bootstrapping.) Initial conditions for the three runs were the same. Figures 3(a) to (c) correspond to dead-band widths of 2.0, 3.0, and 4.0 psi, respectively. A trend toward less oscillatory response is seen in going from the 2.0-psi (1.4-N/cm^2) dead-band run to the runs with larger dead-band widths. The 2.0-psi (1.4-N/cm^2) dead-band run shows a considerably more oscillatory response than the 3.0-psi (2.1-N/cm^2) run. The 4.0-psi (2.8-N/cm^2) dead-band run was slightly less oscillatory than the 3.0-psi (2.1-N/cm^2) run; all remaining runs were made using a 4.0-psi (2.8-N/cm^2) dead-band.

In figure 4 mercury-condensing-pressure plots for startup runs with three different NaK flow-control valve gains are shown; the pressure dead-band width used was 4.0 psi (2.8 N/cm^2). All other parameters and the initial conditions are the same as for the runs of figure 3. Figure 4(a) to (c) correspond to valve gains of 3.2, 6.4, and 12.8 percent per second, respectively. A trend toward more oscillatory response of condensing pressure is seen in going from the lowest-gain run to the runs with larger gains. The run made with a valve gain of 12.8 shows a much more oscillatory response than the 6.4-gain run. The 3.2 run is slightly less oscillatory than the 6.4 run, but shows more overshoot of the upper dead-band. It might be desirable to tolerate more oscillations with the 6.4 gain in order to get less overshoot than that observed with the 3.2 gain. The remaining runs discussed in this report were made using a valve gain of 6.4 percent per second.

The six plots of condensing pressure previously discussed are identical up to the point at which the pressure exceeds the upper dead-band limit for the first time.

Effect of Initial NaK Flow

The control parameter, initial condenser NaK flow, could be made high enough to eliminate the initial overshoot. If this parameter is made too high, however, the condensing pressure (and the mercury pump NPSH) will be too low at the end of mercury injection. The runs discussed allow an approximate determination of the highest initial condenser NaK flow consistent with adequate NPSH at the end of mercury injection (for the given Hg ramp rate and condenser inventory).

In figure 5 mercury-condensing pressure for startup runs with three different initial NaK flows are shown; the valve gain used was 6.4 percent change in flow per second.

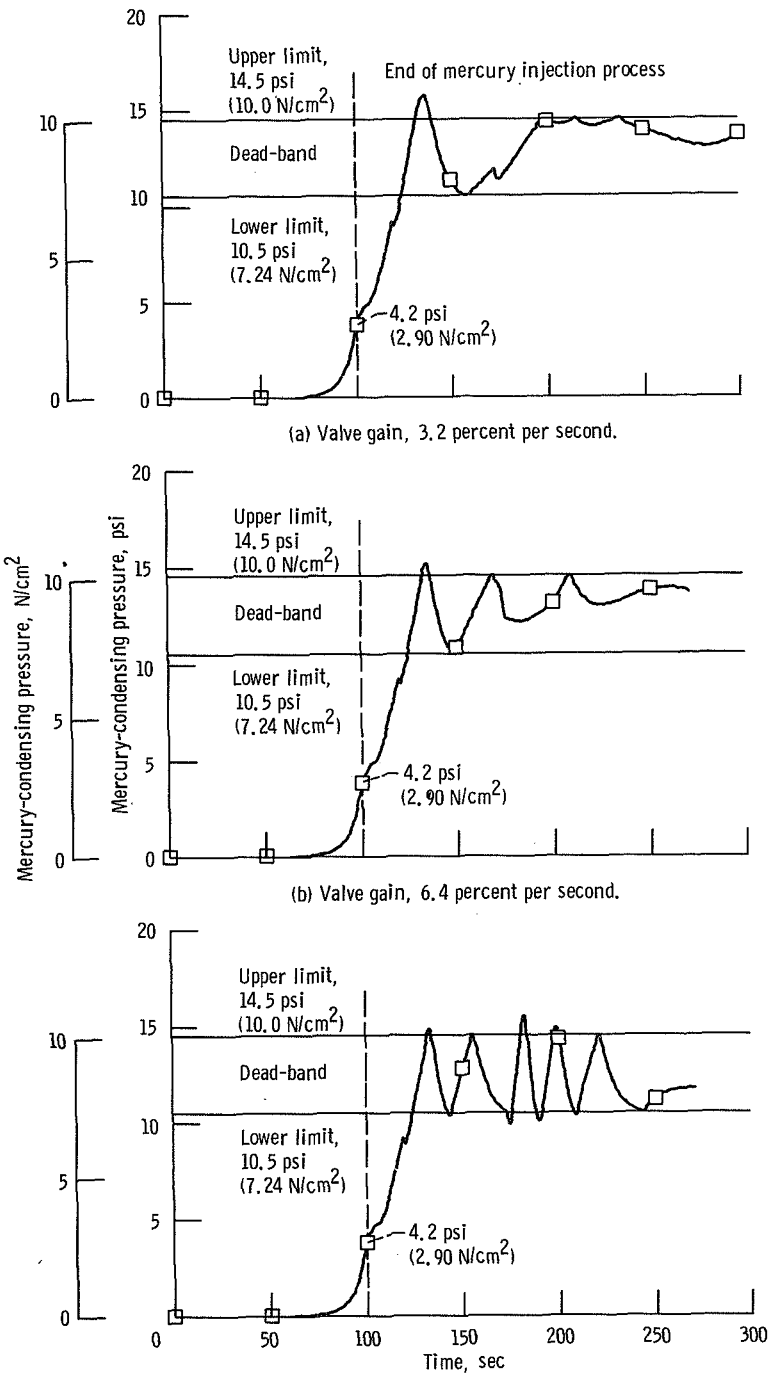

(c) Valve gain, 12.8 percent per second.

Figure 4. - Effect of valve gain on control response. Pressure dead-band width, 4 psi (2.8 N/cm^2); initial condenser coolant flow, 18 percent of design flow (after bootstrapping); final condenser inventory, 40 pounds mass (18.2 kg); slow mercury flow schedule (100-sec ramp).

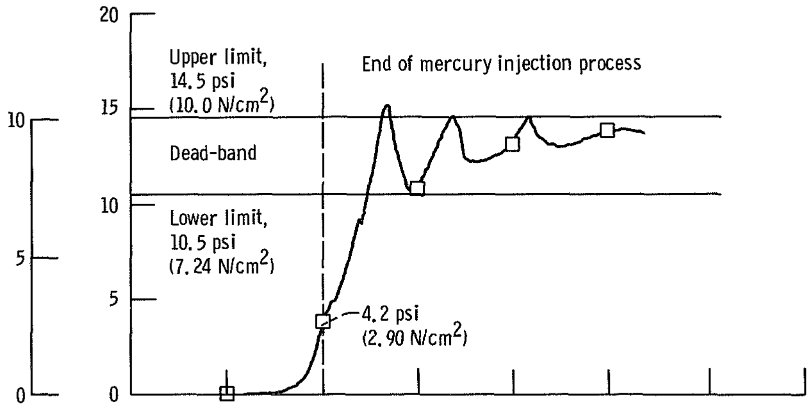

(a) Initial condenser coolant flow, 18 percent of design flow (after bootstrapping).

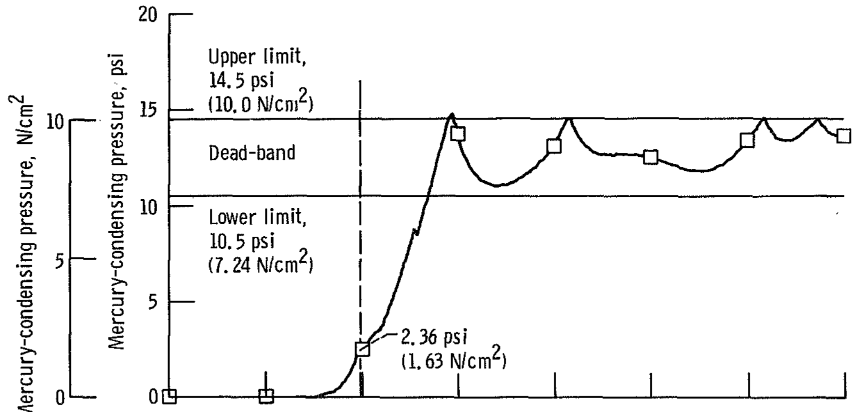

(b) Initial condenser coolant flow, 20 percent of design flow (after bootstrapping).

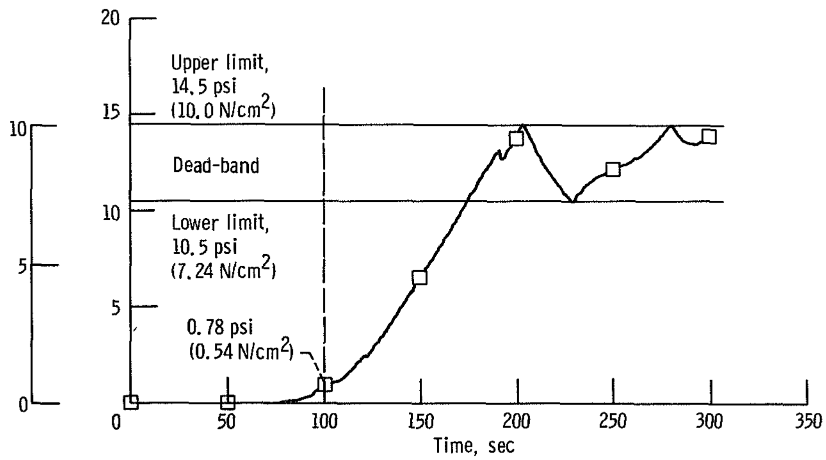

(c) Initial condenser coolant flow, 25 percent of design flow (after bootstrapping).

Figure 5. - Effect of initial condenser coolant flow on control response. Valve gain, 6.4 percent per second; pressure dead-band width, 4 psi (2.8 N/cm^2); final condenser inventory, 40 pounds mass (18.2 kg); slow mercury flow schedule (100-sec ramp).

All other parameters are the same as for figure 4. The heat-rejection-loop initial temperatures were not changed when the initial NaK flow was changed. The initial NaK flow mentioned here corresponds to the initial HRL temperatures and is one-half of the "initial" NaK flow at design pump speed. (In a real situation, maintaining the same radiator exit temperature and increasing the flow through the condenser from 9 to 10 percent of design while maintaining a 38-kW heat-rejection level implies a drop in radiator inlet temperature from 230° to 222° F (373 to 369 K). These conditions imply a radiator 2 percent larger in area.) Therefore, the initial conditions used, with the exception of the initial NaK flow, were the same as for the previous runs. Figures 5(a) to (c) correspond to initial NaK flows (at design pump speed) of 18, 20, and 25 percent of design HRL flow, respectively. Changing the initial NaK flow from 18 to 20 percent of the design flow reduces the pressure overshoot of the upper dead-band. However, the pressure level at the end of mercury injection is smaller for the 20-percent than for the 18-percent initial flow case. A further increase in initial NaK flow to 25 percent of the design value reduces the condensing pressure level at the end of injection to about 0.78 psi (0.54 N/cm^2). From figure 6 the required minimum NPSH at 53.5 percent of design mercury flow is 1.0 psi (0.69 N/cm^2). Therefore, a condensing pressure this low should be expected to result in mercury pump cavitation. The 20-percent initial NaK flow case yields a condensing pressure of 2.36 psi (1.63 N/cm^2) at the end of mercury injection. This pressure is 1.36 psi (0.94 N/cm^2) above the minimum required NPSH and is therefore adequate. However, to provide more NPSH margin at the end of injection it may be desirable to tolerate slightly more overshoot and use an initial NaK flow of 18 percent of design. For the 18-percent initial NaK flow case, the pressure at the end of injection is 3.2 psi (2.2 N/cm^2) above the minimum required NPSH.

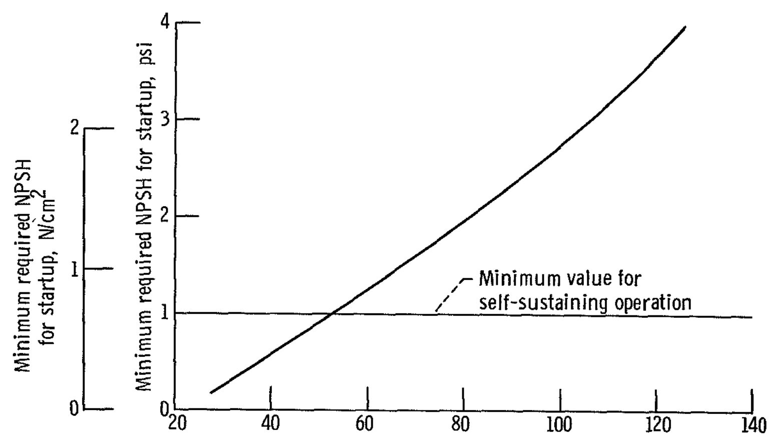

Figure 6. - Minimum required net positive suction head (NPSH) for mercury pump as function of design mercury flow rate.

Effect of Mercury Condenser Inventory and Mercury Flow Rate Schedule

Condenser mercury inventory and the mercury flow rate schedule are system characteristics which are determined primarily by conditions outside the condenser. Condenser inventory is uncertain, even when a fixed inventory is injected into the system, for the following reasons:

(1) Condenser mercury inventory is dictated by boiler inventory. Boiler heat-transfer rate, and therefore boiler inventory, is very sensitive to contaminants on the inner surfaces of the boiler tubes.

(2) When the system is restarted, the amount of mercury remaining in the system since the previous shutdown cannot be accurately determined.

Mercury ramp rate is dictated primarily by other system considerations. Ramps of duration much less than 40 seconds do not appear advisable from the viewpoint of reactor temperature transients. Very long ramps (150 sec or longer) can result in the application of electrical load (pumps, control components) while mercury flow, and therefore applied turbine torque, is too low to accomplish bootstrapping. Even so, acceptable range of these inputs may be limited by condenser-pressure control requirements. The runs discussed in this section allow evaluation of the control performance over ranges of mercury inventory and mercury flow ramp rate.

Runs made with ranges of condenser inventories are shown in figures 7 and 8. The slow mercury flow rate schedule (100-sec ramp) was used for the runs in figure 7 and a fast mercury flow rate schedule (40-sec ramp) was used for the runs shown in figure 8. Initial NaK flow rate through the condenser of 20 percent of design flow (after bootstrapping) and a flow-control-valve gain of 6.4 percent change in flow per second were used.

The condensing pressure during startup is seen to be very sensitive to changes in condenser inventory. For the runs shown in figure 7 (100-sec Hg ramp) the pressure at the end of injection is seen to be 0.33 psia (0.23 N/cm^2) for the smallest inventory of 17 pounds (7.7 kg). Increasing the inventory to 40 pounds (18 kg) raises the pressure at the end of injection to 2.4 psia (1.6 N/cm^2) as seen in figure 9(b). Condensing pressure at the end of injection is shown as a function of condenser inventory in figure 9 for both the 100-second ramps of figure 7 and for the 40-second ramps of figure 8.

From figures 7 to 9 it is possible to determine acceptable ranges of condenser inventory for the fast and slow mercury flow rate schedules. Approximate minimum inventories for each of the two ramp rates may be determined from figure 9. For the 40-second mercury ramp the end of the injection process always occurred after the mercury flow had reached 53.5 percent of the design flow. From figure 6 the minimum required NPSH at 53.5 percent of design flow is 1.0 psia (0.69 N/cm^2). For the smallest inventories used with the 100-second ramp, the injection process ended before

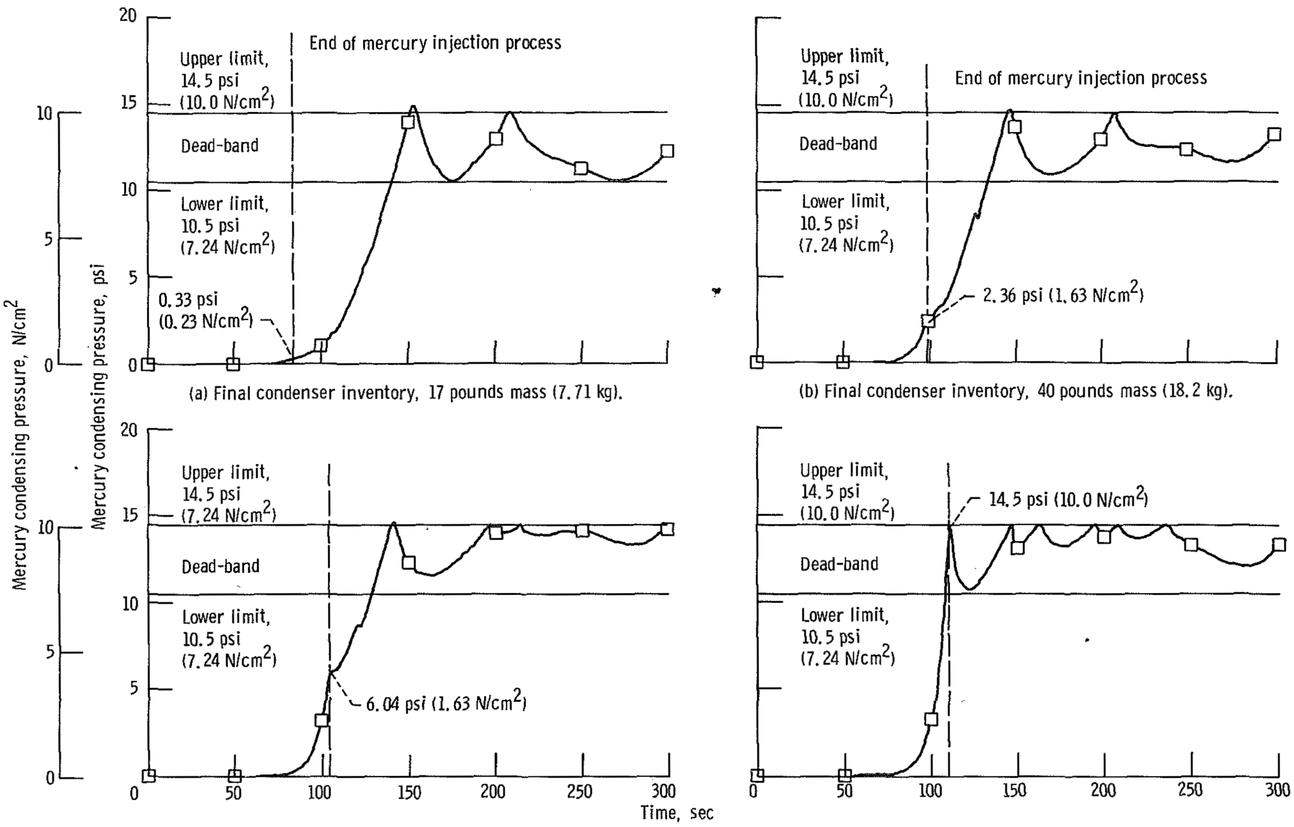

(a) Final condenser inventory, 17 pounds mass (7.71 kg).

(b) Final condenser inventory, 40 pounds mass (18.2 kg).

(c) Final condenser inventory, 53 pounds mass (24.0 kg).

(d) Final condenser inventory, 64 pounds mass (29.0 kg).

Figure 7. - Effect of condenser inventory on control response for slow mercury flow schedule. Valve gain, 6.4 percent per second; pressure dead-band width, 4 psi (2.8 N/cm²); initial condenser coolant flow, 20 percent of design flow (after bootstrapping); slow mercury flow schedule (100-sec ramp).

completion of the mercury ramp. However, the lowest flow level at which injection ended was 45 percent of design. The minimum mercury pump NPSH required at 45 percent of design flow is 0.75 psia (0.52 N/cm^2), or very close to 1.0 psia (0.69 N/cm^2), as seen from figure 6. Therefore, assuming a minimum required NPSH of 1.0 psia (0.6 N/cm^2) for both ramp rates, minimum required inventories for both rates may be determined from figure 9. Minimum inventory for the 40-second ramp is 25 pounds (11 kg) and for the 100-second ramp is 30 pounds (14 kg).

Inventory maximums are dictated by initial pressure overshoots of the upper dead-band. By comparison of figures 8(d) and (e), 60 pounds (27 kg) appears a reasonable approximation of the maximum allowable inventory for the 40-second ramp. Figure 7(d) shows that a 64-pound (29-kg) inventory would be acceptable for the 100-second ramp and even a few more pounds (kg) would probably be acceptable.

Therefore, for a 40-second mercury ramp a 35-pound (16-kg) range of inventories from 25 pounds (11 kg) to 60 pounds (27 kg) is acceptable. For a 100-second mercury ramp at least a 35-pound (30-kg) range from 30 pounds (14 kg) to 65 pounds (30 kg)

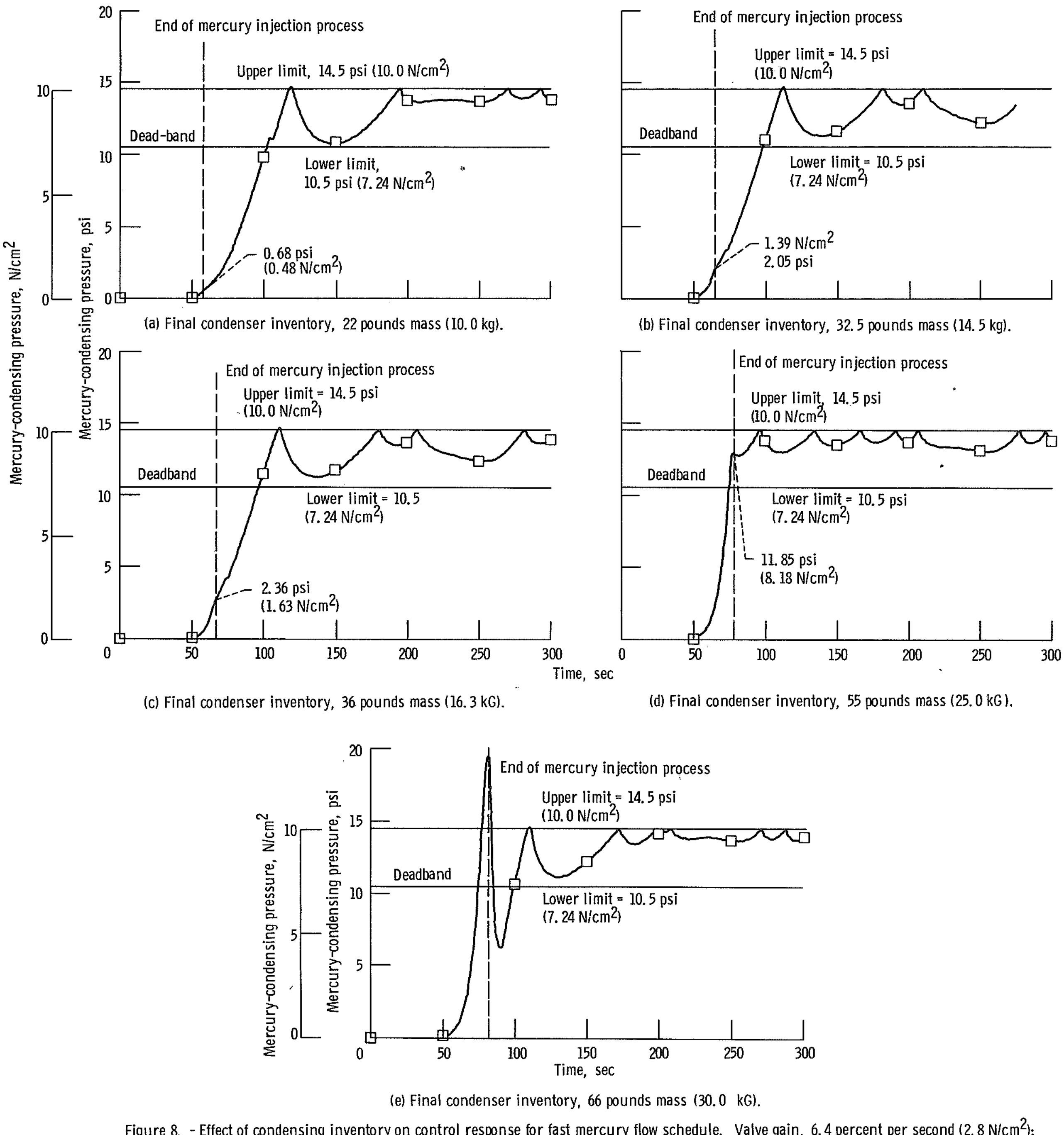

Figure 8. - Effect of condensing inventory on control response for fast mercury flow schedule. Valve gain, 6.4 percent per second (2.8 N/cm^2); pressure dead-band width, 4 psi (2.8 N/cm^2); initial condenser coolant flow, 10 percent of design flow (before bootstrapping); fast mercury flow schedule (40-sec ramp).

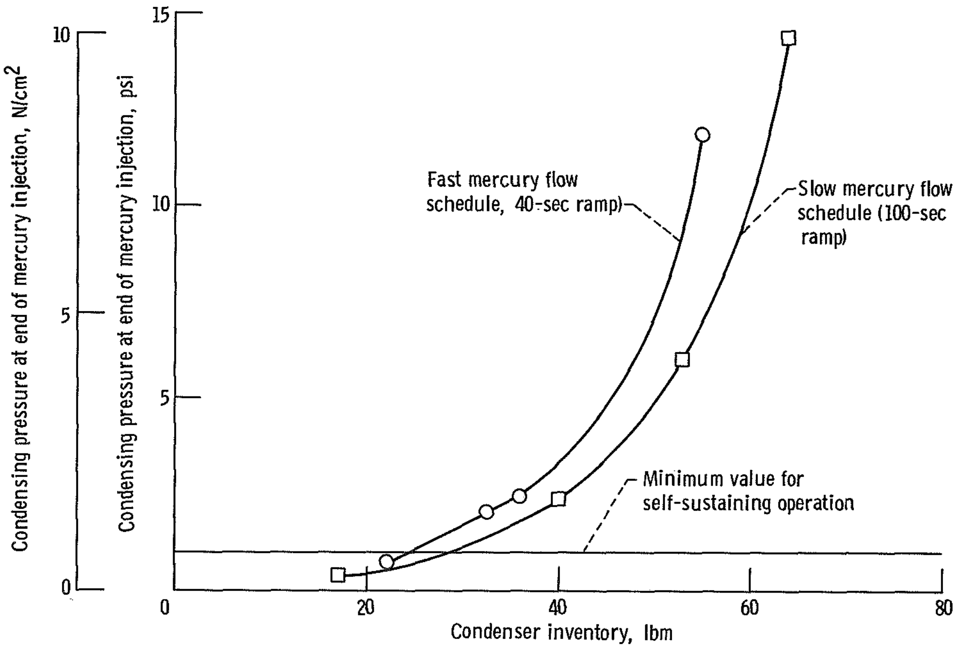

Figure 9. - Condensing pressure at end of mercury injection as function of condenser inventory.

appears acceptable. It also follows that any mercury ramp between 40 and 100 seconds would probably be acceptable for inventories in the 30-pound (14-kg) range from 30 pounds (14 kg) to 60 pounds (27 kg).

SUMMARY OF RESULTS

The results from a study of a dead-band condensing-pressure control for SNAP-8 startup can be summarized as follows:

(1) Control response becomes more oscillatory as dead-band width is decreased. Response goes from a non-limit-cycling to a limit-cycling form for widths between 3.0 psi (4.1 N/cm^2) and 2.0 psi (1.4 N/cm^2).

(2) Control response becomes more oscillatory as the valve gain is increased. Response goes from a non-limit-cycling to a limit-cycling form for valve gains between 6.4 and 12.8 percent per second.

(3) Increasing the initial NaK flow decreases the initial overshoot but also decreases the mercury pump NPSH during startup. Mercury pump NPSH goes from adequate to inadequate when initial NaK flow is increased from 20 to 25 percent of design. An 18-percent initial NaK flow gives a more comfortable NPSH margin than a 20-percent initial NaK flow and still has an acceptable initial pressure overshoot of the upper dead-band limit.

(4) There is a limited range of condenser inventories for which control performance is satisfactory. Satisfactory performance was obtained over a 35-pound (16-kg) range for both mercury flow ramps. The satisfactory range extended from 25 pounds (11 kg) to 60 pounds (27 kg) for the 40-second ramp and from 30 pounds (14 kg) to 65 pounds (29 kg) for the 100-second ramp.

(5) It follows from (4) that mercury flow ramps to the system self-sustaining level from 40 to 100 seconds in length should yield satisfactory performance provided condenser inventory is in the corresponding 35-pound (16-kg) range. It also follows that if the inventory is restricted to the 30-pound (14-kg) range from 30 pounds (14 kg) to 60 pounds (27 kg), all ramps from 40 to 100 seconds in length should yield satisfactory performance.

Lewis Research Center,
National Aeronautics and Space Administration,
Cleveland, Ohio, November 20, 1969,
120-27.

APPENDIX A

SNAP-8 CONDENSER SIMULATION

The SNAP-8 condenser is illustrated in figure 10; the simulation follows. Symbols are given in appendix B. For simplification the following assumptions are made:

(1) Condenser heat transfer along the flow axis is negligible.

(2) A mean diameter can be used for all calculations, which equals $1/2(\text{Diam}_{\text{inlet}} + \text{Diam}_{\text{outlet}})$.

(3) The heat capacity of the tubes can be added to the heat capacity of the NaK.

(4) Condensing takes place right from the beginning of the condenser (i.e., no superheat region).

(5) The heat-transfer area is 73 times the heat-transfer area for one tube.

With these assumptions, the condenser can be considered to be a simpler tube-in-tube condenser, as shown in figure 11.

The condenser is divided into 40 equal segments or lumps (41 nodes) and is considered to be made up of two main regions: the condensing region and the liquid region

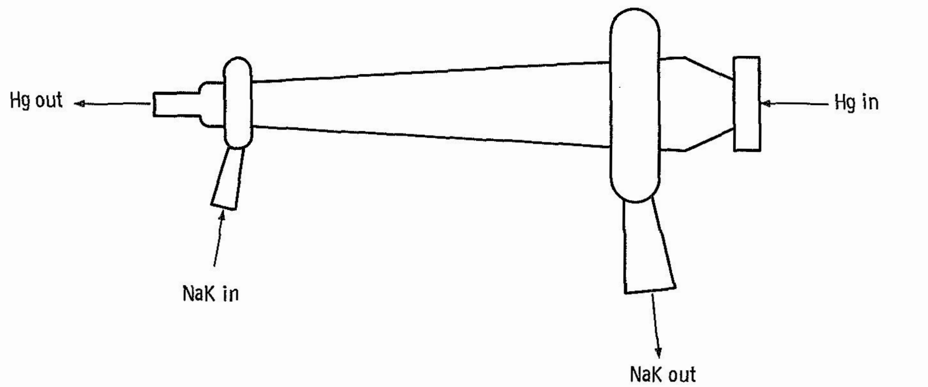

Figure 10. - SNAP-8 condenser.

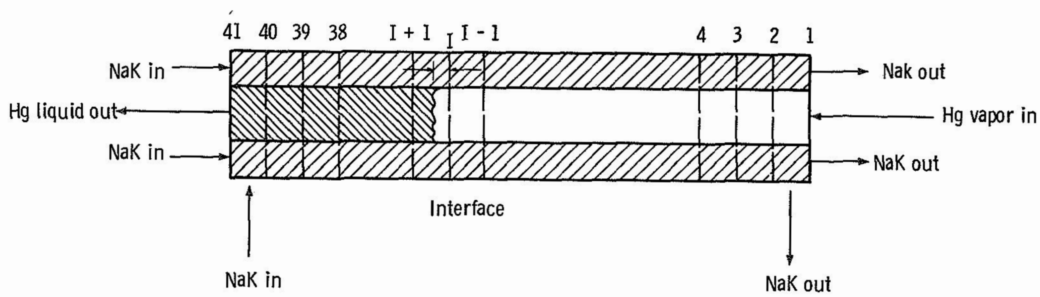

Figure 11. - Simplified condenser model.

(fig. 11). The average NaK temperature for the mercury-condensing region can be calculated as follows:

$$T_{NaK,\,av}\Big|_{\substack{Cond\\region}} = \frac{\displaystyle\sum_{K=1}^{K=I} T_{NaK,\,K}\Big|_{\substack{Cond\\region}} + T_{RI}}{\text{Number of nodes}}$$

where

$$T_{RI} = RI * \frac{\left[T_{NaK}(I+1) + T_{NaK}(I)\right]}{2}$$

(see fig. 12). This assumes that NaK temperature is constant from the last lump

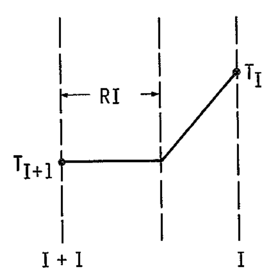

Figure 12. - Location of condenser liquid-vapor interface.

before the interface to the interface. And, with assumption (4), $T_{NaK,\,av}$, and the heat flow into the condenser from the turbine subroutine, Q_{in}, the condensing temperature can now be obtained.

$$Q_{in} = U_c A_c (T_{cond} - T_{NaK,\,av})$$

$$T_{cond} = \frac{Q_{in}}{U_c A_c} + T_{NaK,\,av}$$

It should be noted that $A_c = A_{c,\,initial} \times V_c/V_{c,\,initial}$. Therefore, as the condensing volume V_c changes so does the condensing area A_c.

Having obtained the condensing temperature, the condensing pressure can now be calculated from the Clausius-Clapeyron equation

$$\frac{d(\ln P)}{dT} = \left.\frac{\Delta h}{RT^2}\right|_{T,\,P=\text{constant}}$$

where

Δh heat of vaporization

R specific gas constant

This equation can be used because, for small temperature changes, Δh can be considered constant. With this assumption, the preceding equation can be integrated (ref. 3) as follows:

$$\int_{P_o}^{P} d(\ln P) = \int_{T_o}^{T} \frac{\Delta h}{RT^2}\, dT$$

$$\ln \frac{P}{P_o} = -\frac{\Delta h}{R}\left(\frac{1}{T} - \frac{1}{T_o}\right)$$

$$\ln P = -\frac{1}{T}\frac{\Delta h}{R} + \left(\frac{\Delta h}{RT_o} + \ln P_o\right)$$

$$P = \exp\left(C_1 - \frac{C_2}{T}\right)$$

where

$$C_1 = \frac{\Delta h}{RT_o} + \ln P_o$$

$$C_2 = \frac{\Delta h}{R}$$

And for this case the condensing pressure becomes

$$P_{cond} = 14 - \frac{12\ 890}{T_{cond} + 460}$$

where P_o, T_o correspond to a point on the mercury vapor saturation curve.

The change in the condensing volume with time is calculated from the mass balance equation

$$\frac{dV_c}{dt} = \Delta W_{Hg} \nu_{Hg}$$

$$\frac{dV_c}{dt} = - \left[(W_{Hg})_{vapor} - (W_{Hg})_{liquid} \right] \nu_{Hg}$$

Approximating this differential over a finite time interval Δt yields

$$(V_c)_{new} = (V_c)_{old} + \frac{dV_c}{dt} (\Delta t)$$

$$(V_c)_{new} = (V_c)_{old} + \left[(W_{Hg})_{vapor} - (W_{Hg})_{liquid} \right] \nu_{Hg} (\Delta t)$$

The temperature at each node in the condensing region can be set equal to the condensing temperature

$$T_{Hg,K} = T_{cond} \qquad K = 1, 2, 3, \ldots, I$$

The temperature of the mercury at each node K in the liquid region can be calculated as follows:

$$\frac{\partial \left[\rho_{Hg} (Cp)_{Hg} T_{Hg,K} \right]}{\partial t} = \frac{\partial \left[\rho_{Hg} v_{Hg} (Cp)_{Hg} T_{Hg,K} \right]}{\partial X} + \frac{U_l (\Delta T_K)(dA_{HT})}{(dV_l)}$$

Assuming ρ_{Hg}, $(Cp)_{Hg}$, and v_{Hg} are constant with respect to distance along the condenser, and approximating this differential over a finite interval ΔX, which is equal to one lump, results in

$$\frac{d\,T_{Hg,K}}{dt} = \frac{\rho_{Hg} v_{Hg} (Cp)_{Hg} (T_{Hg,K+1} - T_{Hg,K})}{\rho_{Hg} (Cp)_{Hg} (\Delta X)} + \frac{2U_l \pi r_{HT} (\Delta X)(\overline{\Delta T}_{\Delta K})}{(Cp)_{Hg} \rho_{Hg} \pi r^2 (\Delta X)}$$

where

$$K = I + 1,\ I + 2,\ .\ .\ .\ ,\ 40$$

$$\overline{\Delta T}_{\Delta K} = \frac{1}{2}\left[(T_{NaK,K+1} + T_{NaK,K}) - (T_{Hg,K+1} - T_{Hg,K})\right]$$

For numerical stability, ΔX should always be less than $v_{Hg}(\Delta t)$. When this is true, this differential equation can be approximated over a finite time interval Δt as follows:

$$(T_{Hg,K})_{new} = (T_{Hg,K})_{old} + \frac{d\,T_{Hg,K}}{dt}(\Delta t)$$

where

$$\frac{d\,T_{Hg,K}}{dt} = \frac{v_{Hg}}{\Delta X}(T_{Hg,K+1} - T_{Hg,K}) + \frac{2U_l r_{HT}}{r^2 \rho_{Hg} (Cp)_{Hg}}\ \overline{\Delta T}_{\Delta K}$$

when $(W_{Hg})_{liquid} = 0$,

$$(T_{Hg,K})_{new} = (T_{Hg,K})_{old} + \frac{2U_l r_{HT} (\Delta t)(\overline{\Delta T}_{\Delta K})}{r^2 \rho_{Hg} (Cp)_{Hg}}$$

In the digital program:

(1) $Q_K = \dfrac{2U_l r_{HT} (\Delta t)(\overline{\Delta T}_{\Delta K})}{r^2 \rho_{Hg} (Cp)_{Hg}}$

And for the lump containing the interface

$$(2)\ Q_K = RI \times Q_K + \frac{(T_{cond} - T_{Hg,K})(1. - RI)\, U_l}{U_c}$$

$$(3)\ T_{Hg,K+1} = T_{cond}$$

The temperature at each node K of the NaK and tubes can now be obtained

$$\frac{\partial\left[\alpha (Cp)_{NaK}\, \rho_{NaK} T_{NaK,K}\right]}{\partial t} = \frac{\partial\left[\rho_{NaK} v_{NaK} (Cp)_{NaK}\, T_{NaK,K}\right]}{\partial X} + U(\Delta T_K)\, \frac{d A_{HT}}{d V_{NaK}}$$

where α is a factor to add the effect of the tubes, that is, $(Cp)_{effective}/(Cp)_{NaK} = \alpha$. Again assuming ρ_{NaK}, $(Cp)_{NaK}$, and v_{NaK} are constant and approximating over a finite length ΔX which is equal to the length of one lump, the differential equation above can be simplified as

$$\frac{dT_{NaK,K}}{dt} = \frac{\rho_{NaK} v_{NaK} (Cp)_{NaK}\, (T_{NaK,K} - T_{NaK,K+1})}{\alpha \rho_{NaK} (Cp)_{NaK}\, (\Delta X)} + \frac{2 U r_{HT} \pi (\Delta X)(\overline{\Delta T}_{\Delta K})}{\dfrac{\alpha W_{NaK}}{40}}$$

where K = 1, 2, 3, . . ., 40. And for a finite time interval Δt the equation becomes

$$(T_{NaK,K})_{new} = (T_{NaK,K})_{old} + \frac{dT_{NaK,K}}{dt}\, (\Delta t)$$

where

$$\frac{dT_{NaK,K}}{dt} = \frac{v_{NaK}}{\alpha (\Delta X)}\, (T_{NaK,K} - T_{NaK,K+1}) + \frac{2 U r_{HT} \pi L (\overline{\Delta T}_K)}{\alpha W_{NaK}}$$

In the digital program

$$\frac{Q_K \rho_{Hg} (Cp)_{Hg} r^2 \pi L}{\alpha\, W_{NaK}} = \frac{2 U r_{HT} L (\overline{\Delta T}_K)}{\alpha W_{NaK}}$$

APPENDIX B

SYMBOLS

A_c	heat-transfer area for condensing region, ft^2; m^2
A_{cs}	cross-sectional flow area in mercury condenser tubes, ft^2; m^2
A_{HT}	heat-transfer area, ft^2; m^2
$(Cp)_{effective}$	effective specific heat of third-loop fluid when tubes are lumped with third-loop fluid
$(Cp)_{Hg}$	specific heat of liquid mercury, Btu/(lbm)(^oF); J/(kg)(K)
$(Cp)_{NaK}$	specific heat of NaK, Btu/(lbm)(^oF); J/(kg)(K)
$(Cp)_t$	specific heat of tubes in condenser, Btu/(lbm)(^oF); J/(kg)(K)
Δh	heat of vaporization for small temperature changes, Btu/lbm; J/kg
I	node just before condenser liquid-vapor interface (I is in condensing region)
P	pressure, psi; N/m^2
P_{cond}	condensing pressure, psi; N/m^2
P_o	initial pressure (corresponds to a point on mercury vapor saturation curve), psi; N/m^2
Q_{in}	heat flow into condenser from turbine, Btu/(lbm)(sec); J/(kg)(sec)
Q_k	change in mercury temperature at k^{th} node due to conduction which would result during time interval Δt if there were no convection heat flow, ^oF; K
R	specific gas constant, ft-lbf/(lbm)(^oR); m-N/(kg)(K)
RI	fraction of lump in condensing region
r	mean inside radius of condenser tubes, ft; m
r_{HT}	mean heat-transfer radius of condenser tubes, ft; m
T	temperature, ^oF; K
T_{cond}	condensing temperature, ^oF; K
$T_{Hg,K}$	temperature of mercury at node K, ^oF; K
T_{NaK}	NaK temperature, ^oF; K

$T_{NaK,av}$	average temperature of NaK for mercury condensing region, ^{o}F; K
$T_{NaK,K}$	NaK temperature at k^{th} node, ^{o}F; K
T_o	initial temperature (corresponds to point on mercury vapor saturation curve), ^{o}F; K
T_{RI}	temperature at condenser liquid-vapor interface, ^{o}F; K
$(\overline{\Delta T})_{\Delta K}$	average temperature difference between NaK and mercury for one lump (K to K + 1) in condenser, ^{o}F; K
ΔT_K	temperature difference between NaK and mercury at node K, ^{o}F; K
t	time, sec
Δt	small increment of time, sec
U	overall heat-transfer coefficient ($U = U_c$ in condensing region and $U = U_l$ in liquid region of condenser), Btu/(sec)(^{o}F)(ft^2); J/(sec)(K)(m^2)
U_c	overall heat-transfer coefficient in condensing region, Btu/(sec)(^{o}F)(ft^2); J/(sec)(K)(m^2)
U_l	overall heat-transfer coefficient in mercury liquid region of condenser, Btu/(sec)(^{o}F)(ft^2); J/(sec)(K)(m^2)
V_c	total volume of mercury vapor in condensing region, ft^3; m^3
V_{NaK}	volume of NaK in condenser, ft^3; m^3
V_l	total volume of mercury in liquid region of condenser, ft^3; m^3
v_{Hg}	velocity of liquid mercury out of condenser, ft/sec; m/sec
V_{NaK}	velocity of NaK through condenser, ft^3; m^3
W_{NaK}	weight of NaK in condenser, lbm; kg
W_t	weight of tubes in the condenser, lbm; kg
$w_{Hg,\ liquid}$	mercury liquid flow rate out of condenser, lbm/sec; kg/sec
$w_{Hg,\ vapor}$	mercury vapor flow rate into condenser, lbm/sec; kg/sec
w_{NaK}	NaK flow rate through condenser, lbm/sec; kg/sec
Δw_{Hg}	difference in flow rates into and out of condenser lbm/sec; kg/sec
X	distance or position, ft; m
α	ratio of effective specific heat of NaK and tubes to specific heat of NaK
ν_{Hg}	specific volume of mercury, ft^3/lbm; m^3/kg

ρ_{Hg}	specific gravity of liquid mercury, lbm/ft^3; kg/m^3
ρ_{NaK}	specific gravity of NaK, lbm/ft^3; kg/m^2

REFERENCES

1. Packe, Donald R.; Schoenberg, Andrew A.; Jefferies, Kent S.; and Tew, Roy C.: Analysis of Condensing Pressure Control for SNAP-8 System. NASA TM X-1292, 1966.

2. Soeder, Ronald H.; Curreri, Joseph S.; and Macosko, Robert P.: Performance of a Multitube Single-Pass Counterflow NaK-Cooled Mercury Rankine-Cycle Condenser. NASA TM X-1548, 1968.

3. Obert, Edward F.; and Gaggioli, Richard A.: Thermodynamics. Second ed., McGraw-Hill Book Co., Inc., 1963.

NASA-Langley, 1970 —— 22 E-5384

NATIONAL AERONAUTICS AND SPACE ADMINISTRATION
WASHINGTON, D.C. 20546

OFFICIAL BUSINESS

FIRST CLASS MAIL

POSTAGE AND FEES PAID
NATIONAL AERONAUTICS AND
SPACE ADMINISTRATION

POSTMASTER: If Undeliverable (Section 158 Postal Manual) Do Not Return

"The aeronautical and space activities of the United States shall be conducted so as to contribute . . . to the expansion of human knowledge of phenomena in the atmosphere and space. The Administration shall provide for the widest practicable and appropriate dissemination of information concerning its activities and the results thereof."

—NATIONAL AERONAUTICS AND SPACE ACT OF 1958

NASA SCIENTIFIC AND TECHNICAL PUBLICATIONS

TECHNICAL REPORTS: Scientific and technical information considered important, complete, and a lasting contribution to existing knowledge.

TECHNICAL NOTES: Information less broad in scope but nevertheless of importance as a contribution to existing knowledge.

TECHNICAL MEMORANDUMS: Information receiving limited distribution because of preliminary data, security classification, or other reasons.

CONTRACTOR REPORTS: Scientific and technical information generated under a NASA contract or grant and considered an important contribution to existing knowledge.

TECHNICAL TRANSLATIONS: Information published in a foreign language considered to merit NASA distribution in English.

SPECIAL PUBLICATIONS: Information derived from or of value to NASA activities. Publications include conference proceedings, monographs, data compilations, handbooks, sourcebooks, and special bibliographies.

TECHNOLOGY UTILIZATION PUBLICATIONS: Information on technology used by NASA that may be of particular interest in commercial and other non-aerospace applications. Publications include Tech Briefs, Technology Utilization Reports and Notes, and Technology Surveys.

Details on the availability of these publications may be obtained from:

SCIENTIFIC AND TECHNICAL INFORMATION DIVISION

NATIONAL AERONAUTICS AND SPACE ADMINISTRATION

Washington, D.C. 20546